

Contribution to the Development of a Reconfigurable and Low-Cost Multistandard Software Defined Radio Transceiver for the New Radio

Michel Mfeze

Research Scholar,

Department of Electrical and Telecommunications
Engineering, National Advanced School of Engineering,
University of Yaounde I, Cameroon

Emmanuel Tonye

Professor,

Department of Electrical and Telecommunications
Engineering, National Advanced School of Engineering,
University of Yaounde I, Cameroon

Abstract—A Multistandard and low cost radio transceiver architecture more suited to the new radio and exploiting the possibilities of software defined radio is proposed in this article. The proposed platform integrates a general purpose processor board which can be the Raspberry pi 3B + development board and radio modules like Adalm Pluto and RTL-SDR. The architecture validation is performed on a multipath fading channel model and on real waveforms of three selected radio standards. We generate a baseband waveform that is either a WLAN Modulation and Coding Scheme (MCS), an LTE Reference Measurement Channel (RMC) or a 5G Fixed Reference Channel (FRC) synthesized in MATLAB using the appropriate toolkits, and upload it to a PlutoSDR module for live transmission. Another PlutoSDR or RTL-SDR according to the standard (signal bandwidth) is then used to capture the signal, which is synchronized, decoded and analyzed. For each of the three standards, the transmitter and receiver systems are defined in compliance at the physical layer level with the specifications of the latest 3GPP standards. The performance analysis and evaluation use various diagrams and signal quality measures such as Error Vector Magnitude (EVM), Modulation Error Rate (MER), Adjacent Channel Leakage Ratio (ACLR) as well as timing and frequency offsets.

Keywords—*Software-defined radio, multistandard terminal, EVM, ACLR, MER, multipath, fading channel, WLAN, LTE, 5G NR.*

I. INTRODUCTION

Software-defined radio (SDR) makes it possible to design flexible transceivers architectures, both in frequency and in modulation format, capable of generating waveforms of all standards while respecting the output power level for each and ensuring a good performance. Digital mobile communications systems tend to integrate more and more applications (GSM, radio, TV, GPS, etc.) while operating on multiple standards. This constant and rapid evolution of wireless and communication technologies implies online reconfigurability of receivers using software programming justifying the term software radio with a requirement for increasingly higher data rates and frequency bands. Terminals must then adapt their hardware to suit wireless networks such as GSM, EDGE, UMTS, IEEE 802.11a / b / g, LTE and the booming 5G. This process must be dynamic and requires the receiver to be flexible that is, adaptable and reconfigurable, more or less in

real time without the need to physically modify the hardware [1]. Software reconfigurability involves digitizing signals as close as possible to the antenna [2], because high speeds require large bandwidth.

In conventional transceivers, digital baseband processing is typically performed by dedicated hardware circuits, mostly rigid but power efficient ASICs. Many smartphones and similar devices currently have up to about 8 different radios optimized to receive various signals of different frequency bands and standards. Soon they might even include radios to also receive UHF IoT and TV White Space signals [3]. All this explains the growing interest in low cost multimode terminals based on software radio techniques.

SDR is a radio communication system, which gives the possibility of software control of modulation method, coding scheme, filtering, wideband or narrowband operations, spread spectrum techniques, bandwidth, channel access techniques and waveform requirements [4]. Almost all of the functionality associated with the physical layer (PHY) is implemented in software using digital signal processing (DSP) algorithms.

The concept of software-defined radio was introduced by J. Mitola in the early 1990s [5]. The architecture of SDR systems defines the hardware abstraction layer. When designing an SDR terminal, it is necessary to choose a computing platform for the digital part, a radio front end, and to make a compromise between the sampling frequency, the complexity of the terminal and the energy consumption. The cost functions of the computing platform are programmability, flexibility, power consumption and computing power [6].

ASICs offer the best possible performance at the lowest cost of silicon, but they suffer from a lack of flexibility and a high one-time engineering cost. DSP processors are based on the Harvard architecture, an extension of the Von-Neumann architecture, and are unable to meet SDR speed requirements despite a set of arithmetic and control instructions optimized for signal processing algorithms. Systems on a Chip (SOC) have limited flexibility. FPGAs are dynamically reconfigurable, and these high-performance, programmable

hardware can efficiently perform highly parallel, compute-intensive signal processing functions [7].

For these reasons, most of the existing SDR hardware platforms are built around FPGAs like the USRP2 from Ettus Research LLC, the Rice Wireless Open-Access (WARP) research platform, the Berkeley 3 emulation engine. (BEE3), the University of Kansas Agile Radio (KUAR)., Small Form Factor Software Defined Radio (SSF-SDR) and Intelligent Transportation System (ITS) from NICT.

For software platforms, next to Desktop PC software such as Gqrx, SDR #, HDSDR, PowerSDR, QtRadio, GNU Radio, Matlab-Simulink, OSSIE and WARPnet etc, there are also Android mobile versions like SDR Touch and glSDR as well as a few that provide a web interface like WebSDR and ShinySDR, which can be used for simple remote access to the receiver.

Designing true global SDR receivers for analog and digital communication systems based on advanced DSP and digital communications theory has so far been difficult given the high cost of solutions based on basic FPGAs and SOCs. However, this is now possible with the advent of low-cost hardware such as RTL-SDR or, easy-to-use and programmable Adalm Pluto module, as they can be integrated into technical programming environments such as MATLAB-Simulink the VHDL and other open source solutions. For a multistandard terminal, the ultimate solution would be to use this SDR hardware to digitize and capture all baseband signals at 2.5 or even 3GHz, and to implement all of these receivers in software code [3].

RTL-SDR equipment was released in early 2013 and was sourced from consumer grade DVB-T receivers. It was not originally designed for use as generic programmable SDRs and the switch to the current application is due to the number of independent engineers and developers in the SDR community allowing the device to match over the 25 MHz to 2.3 GHz range, producing 8-bit raw IQ data samples at a programmable baseband sample rate. Shortly after this discovery, the name RTL-SDR was adopted, which referred to the fact that RTL-based (Realtek) DVB receivers could be used as SDR.

Several authors have made various contributions in the field of software-defined radio, some focusing on modular or holistic aspects both at the hardware and software level such as reconfigurability and reusability [8]-[10] and broadband digitization [11][12] as close as possible to the antenna [13], the performance-consumption tradeoff [14][15], the architecture of the receiver [16], the prototyping options [13][11][17], signal processing and quality of service [18]-[21], data security and cryptography [22], as well as the co-design and partitioning techniques [23]. The possibility of designing a universal multistandard mobile phone (GSM, CDMA, TDMA, AMP etc.) capable of self-reconfiguration to adapt to the identified protocol and based on flexible FPGA technology has already been the subject of several works prior to the present work [24]-[26]. Beyond the reconfigurable software radio, some authors are already considering the transition from a management architecture for the configuration of multi-standard software radio systems to a

management architecture for cognitive or intelligent radio [27].

Finally, among the most recent concerns is the development of mono standard or multistandard software radio systems [28] at a lower cost with the advent of processing platforms (Raspberry Pi [29], Panda etc.) and software radio components. (RTL-SDR, Adalm Pluto etc) at low cost by sometimes exploiting the model-based design method [30]

It is in this context that works such as the design of FM [30][31] or AM [30][32] radio receivers intervene or the prototyping of a reconfigurable IEEE 802.11 and ZigBee receiver with a single RF front end operating in the license-free 2.4 GHz ISM band [28], built around FPGAs. The authors of [33] have also worked on a low cost angle of arrival (AoA) estimation unit that can be used as an Internet of Things (IoT) receiver and provides AoA estimates of signals received. The unit uses a series of RTL-SDR dongles. The authors of [34] show how Raspberry Pi boards can be used, together with Simulink, to easily implement an OFDM transceiver.

Software-defined radio systems are a solution to the problem of scalability and reconfigurability of transceivers which can be software modified to adapt to new technologies without compromising the hardware. Nevertheless, the literature shows that the proposed architectures are based on costly and / or complex solutions or else are restricted to limited applications.

II. METHODOLOGY

A. Choice of software-defined radio solution

ASICs are about the only option that can achieve high throughput with reasonable power consumption but offer a limited level of programmability. FPGAs should be considered for high throughput applications which can tolerate slightly higher power consumption but still cost a lot. GPPs can now process low to medium bit rate signals in real time. They offer unmatched flexibility and ease of development. DSPs are based on microprocessor architectures and are programmable in high level languages such as C / C ++ to gain great flexibility. On the other hand, they do not offer a sufficiently high flow or a lower power than that of the alternative options. SPU should be considered on a case-by-case basis. The two main concerns when considering SPU are the longevity of the device and the ease of development.

Three major signal processing architectures can be defined: All-software using a GPP, a GPP with hardware acceleration using an FPGA or an SPU, or an FPGA. GPP is undoubtedly the best maintainability platform because it allows the reusability of codes (C ++ or Java code). On the other hand, a good compromise is a combination of these architectures to achieve optimal energy efficiency while preserving the system requirements for performance and to build a fully reconfigurable system that has the ability to adapt to new hardware elements of the front end architecture and to the analog-to-digital (A/D) and/or digital-to-analog (D/A) conversion of an SDR [12].

Considering all of the above, we are proposing a development with possibilities for a high performance SDR in terms of cost

and power consumption, comprising an available and affordable system of SOC system-on-chip with ARM (Advanced RISC Machine) architecture embedded in a Raspberry Pi 3B + nanocomputer. The proposed SDR platform therefore uses the Raspberry pi 3B + development kit and radio modules: two Adalm Pluto modules or one Adalm Pluto module on the transmitter side and an RTL-SDR on the receiver side. The digital signal processing is initially performed using Matlab / Simulink.

B. Realization of the multistandard software radio terminal architecture

For a multistandard SDR transceiver application, we generate a baseband waveform that is either a WLAN modulation and coding scheme (MCS), an LTE reference measurement channel (RMC), or a 5G fixed reference signal (FRC) synthesized in MATLAB, and upload it to a PlutoSDR module for live transmission. Another PlutoSDR or RTL-SDR according to the standard (signal bandwidth) is then used to capture the signal, which is synchronized, decoded and analyzed in MATLAB. For each of the three standards, the transmitter and receiver of LTE, WLAN and 5G wireless systems are defined in compliance at the physical layer level with the specifications of the latest 3GPP standards.

First, each of the above units is connected to a host computer using the USB 2.0 interface and the complex I/Q samples are transmitted to the host via Ethernet via USB. The host computers of the transmitter and receiver units are running 64-bit Windows 8 operating systems while the PlutoSDR units are running embedded Linux.

In addition, for operation as a stand-alone terminal, the processing algorithms can be integrated into general purpose processors (GPP) based on Raspberry Pi 3B + modules. To achieve this, these algorithms must be compiled in C / C ++ format and downloaded into the Raspberry Pi with a python script in a software graphical interface for a SISO scenario allowing to switch between the three standards. From this graphical interface the user can choose some of the algorithms implemented to see the performance of the transceiver and the data link.

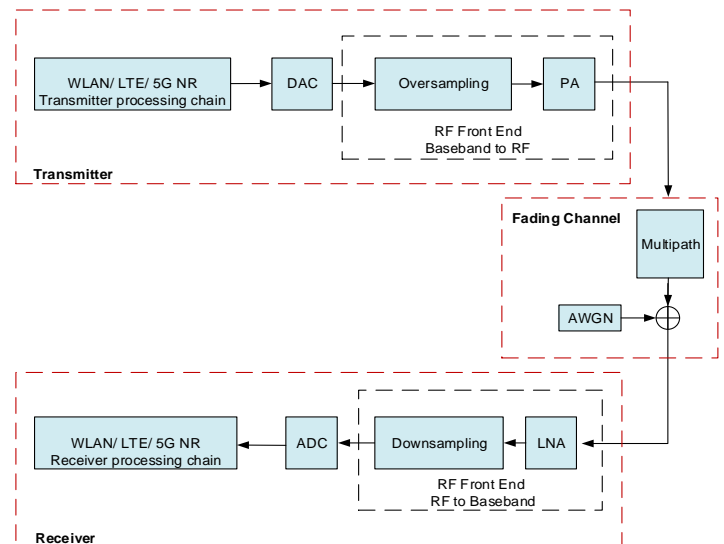


FIG. 1: PROCESSING CHAIN

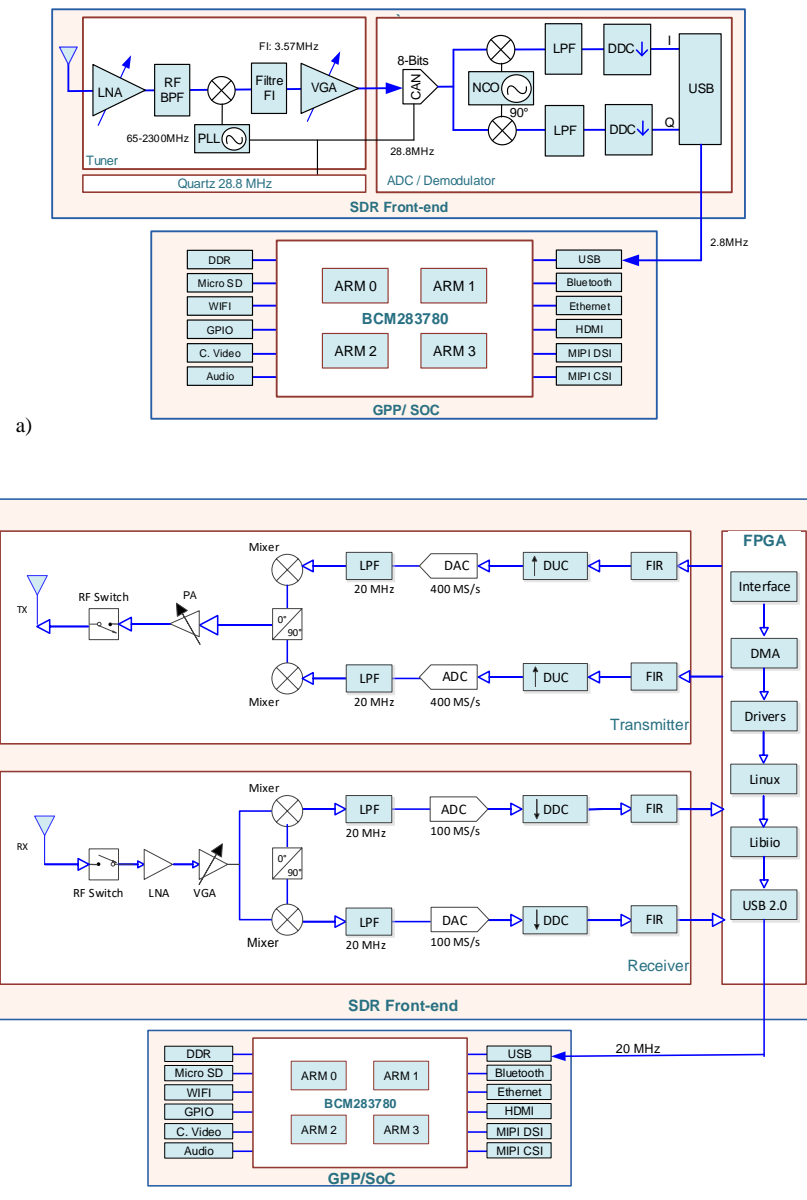


FIG. 2: SDR RECEIVER ARCHITECTURE IS BASED AROUND A GPP LIKE THE RASPBERRY PI 3B+. RF FRONT-END IS PROVIDED BY A) AN RTL-SDR FOR RX ONLY AND B) BY AN ADALM PLUTO MODULE FOR TX/RX.

C. Taking into account the specifications of the MCS, RMC and FRC normative references

A key requirement for the design and verification of radio systems is the ability to work with live signals or even real waveforms. Various standards then define a set of uplink and downlink test pattern waveforms (Modulation and Coding Schemes (MCS) for WLAN [35], RMC Reference Channels for LTE [36], and (FRC) for 5G NR [37][38]) which will therefore be used here for the tests and validation of our receiver. On the other hand, since PlutoSDR and RTL-SDR are SISO devices, no spatial diversity, no beamforming algorithm is needed and therefore no channel and layer mapping. The references retained and used will therefore be limited to the SISO context.

D. Optimization of the multistandard software radio terminal architecture

1) Transmitter optimization by signal filtering to improve ACLR

The transmitted signal is assumed to occupy a given bandwidth, called a channel. All transmission outside of this channel is called out-of-band emission. These should be limited as they create interference on adjacent channels. The maximum level of out-of-band emissions is therefore fixed by the standards of wireless communication systems, in relative value compared to the power emitted on the channel band. The reduction in out-of-band spectral emissions and interference from adjacent channels will therefore be achieved by additional filtering of the signal on emission.



FIG. 3: PRINCIPLE OF THE TRANSMITTER HIGHLIGHTING THE ACLR MEASUREMENT

The ACLR¹ is used as a measure of the amount of power leaking into adjacent channels and is defined as the ratio of the average filtered power centered on the assigned channel frequency to the average filtered power centered on an adjacent channel frequency

$$ACLR = \int_{F_1, F_2} \frac{S(\omega)}{P_\alpha} d\omega = \int_{F_1, F_2} \frac{S(\omega)}{\frac{1}{2}E[|X_k^I|^2]} d\omega \quad (1)$$

$S(\omega)$ is the power spectral density of the transmitted signal. For most communication standards, the most crucial ACLR is that of the first adjacent channel (F_1) and incidentally that of the second F_2 .

$$F_1 = ACLR_1 = \left(\frac{A_0}{A_1}\right)^2 \quad (2)$$

$$F_2 = ACLR_2 = \left(\frac{A_0}{A_2}\right)^2 \quad (3)$$

The minimum ACLR compliance requirements are given for E-UTRA (LTE) and UTRA (W-CDMA) carriers [38]. This is equal to 45dB in most cases.

Filter design

We will use here the Parks-McClellan method which allows to design a constrained optimal order FIR filter with uniform ripple. The filter design parameters for a signal of bandwidth BW and sampling frequency f_s are:

TABLE 1: Filter Design Parameters

Parameter	Value
Type of filter	FIR Lowpass (Parks-McClellan Method)
Sampling frequency	f_s same as for reference signal
Minimum stop band attenuation	80dB > 60dB (3GPP requirement) [39]
Pass band ripple	0.1dB < maximum requirement of 0.2dB
Start of stop band frequency	BW/2
Cut off frequency	90% of stop band start frequency (10% of the Nyquist frequency)

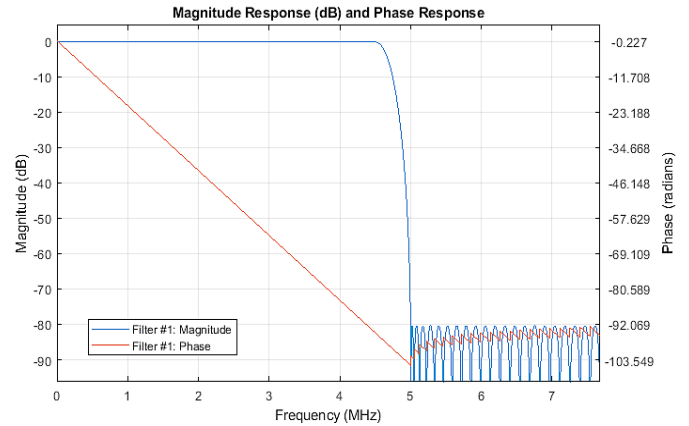


FIG. 4: AMPLITUDE AND PHASE RESPONSE OF THE FILTER

2) Receiver Optimization Using Error Vector Magnitude Analysis

The magnitude of the error vector represents the Euclidean distance between the ideal coordinate of the reference symbol (giving the reference vector R) and the real recorded complex transmitted symbol (giving the measured vector V). The quality of the modulation is specified at the receiver in terms of the magnitude of the error vector for the allocated resource blocks (RB) and the flatness of the spectrum derived from the equalization coefficients generated by the process of EVM measurement

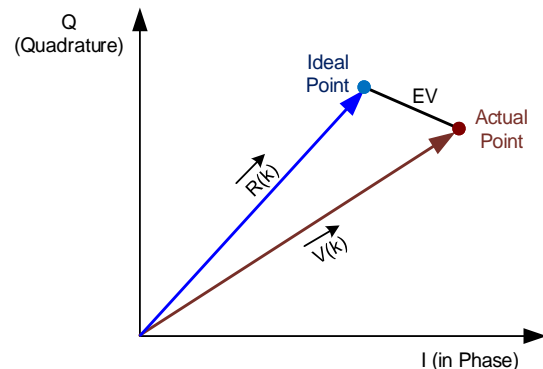


FIG. 5: ILLUSTRATION OF ERROR VECTOR (EV) IN IQ SPACE

$$EVM = \sqrt{\frac{\sum_{k=1}^M |V(k) - R(k)|^2}{\sum_{k=1}^M |R(k)|^2}} \quad (4)$$

$$EVM_{RMS}(\%) = 100 \sqrt{\frac{\frac{1}{N} \sum_{k=1}^N (e_k)}{P_{avg}}} \quad (5)$$

EVM_{RMS} is the root mean square value of EVM across all resource blocks in the LTE signal. The parameter e_k in fact

represents the square of the amplitude of the modulation error vector and is given by:

$$e_k = \delta I_k^2 + \delta Q_k^2 = (I_k - \tilde{I}_k)^2 + (Q_k - \tilde{Q}_k)^2 \quad (6)$$

δI_k and δQ_k are the real part (in phase) and the imaginary part (quadrature) of each modulation error vector.

3) Receiver optimization using modulation error rate

The MER is the ratio between the power of the target symbol and the power of error. The MER is a measure of the SNR in a modulated signal and is a way to quantify the noise of the constellation. The MER in decibels for the K_{th} symbol will be

$$MER_k = 10 \cdot \log_{10} \left(\frac{\frac{1}{N} \sum_{k=1}^N (I_k^2 + Q_k^2)}{e_k} \right) \quad (7)$$

The WLAN, LTE, 5G NR transceiver for SISO communication, are produced using Matlab with the possibility of modifying parameters such as MCS, RMC or FRC which implies a sampling frequency, a modulation (Type and order) etc, as well as the carrier frequency.

TABLE 2: EVM requirements according to 3GPP specifications

Standard	EVM (%)				
	$\pi/2$ BPSK	QPSK	16-QAM	64-QAM	256-QAM
GSM/EDGE	30	9 [8-PSK]	N/A	N/A	N/A
UMTS	30	17.5	12.5	N/A	N/A
LTE	30	17.5	12.5	8	3.5
5G NR	30	17.5	12.5	8	3.5

[40][39][41][42]

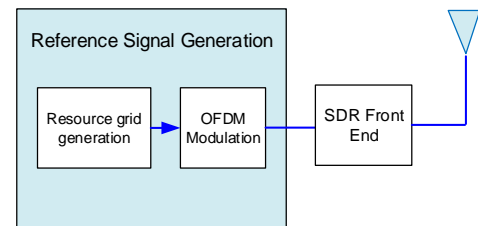


FIG. 6: SYNTHETIC PROCESSING CHAIN OF A TRANSMITTER

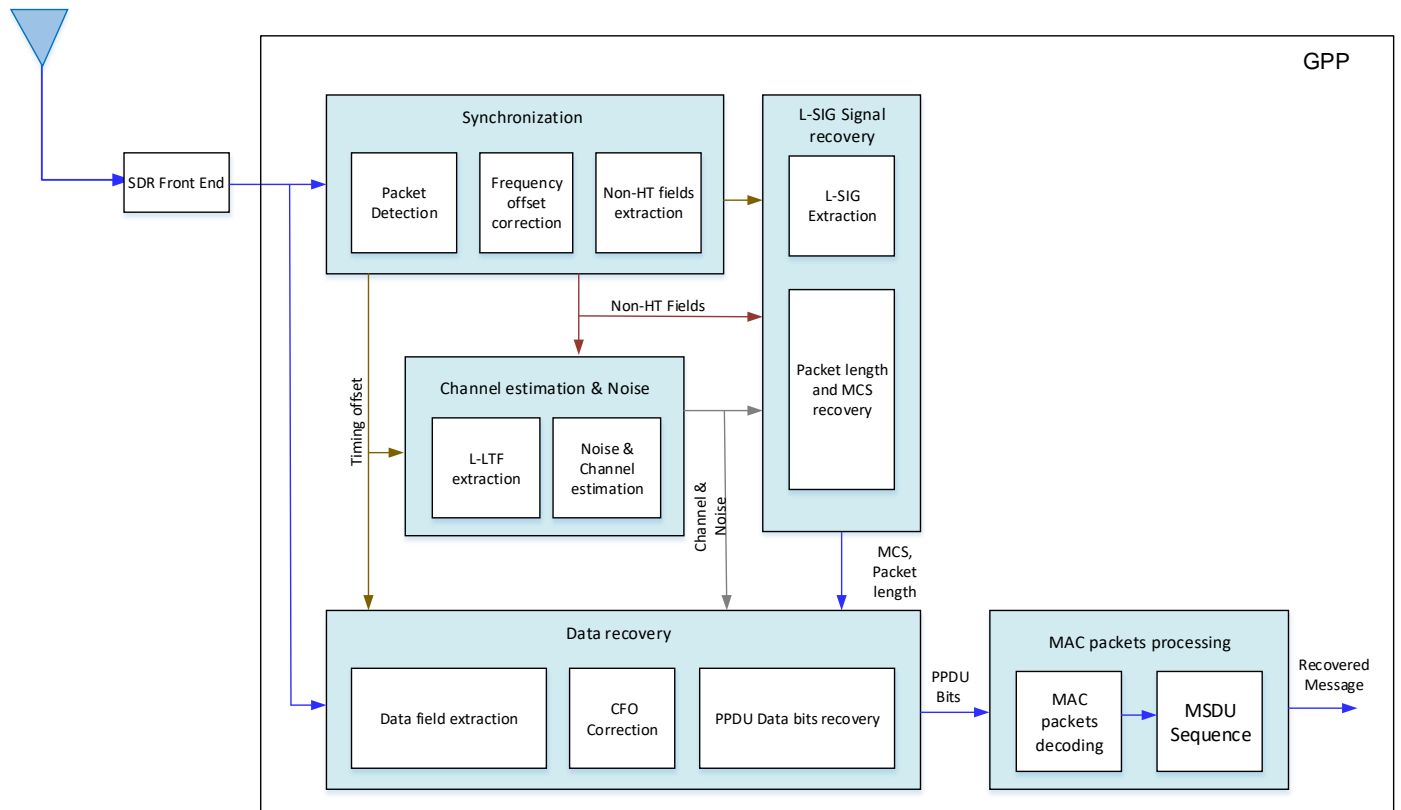


FIG. 7: SYNTHETIC PROCESSING CHAIN OF THE WLAN RECEIVER

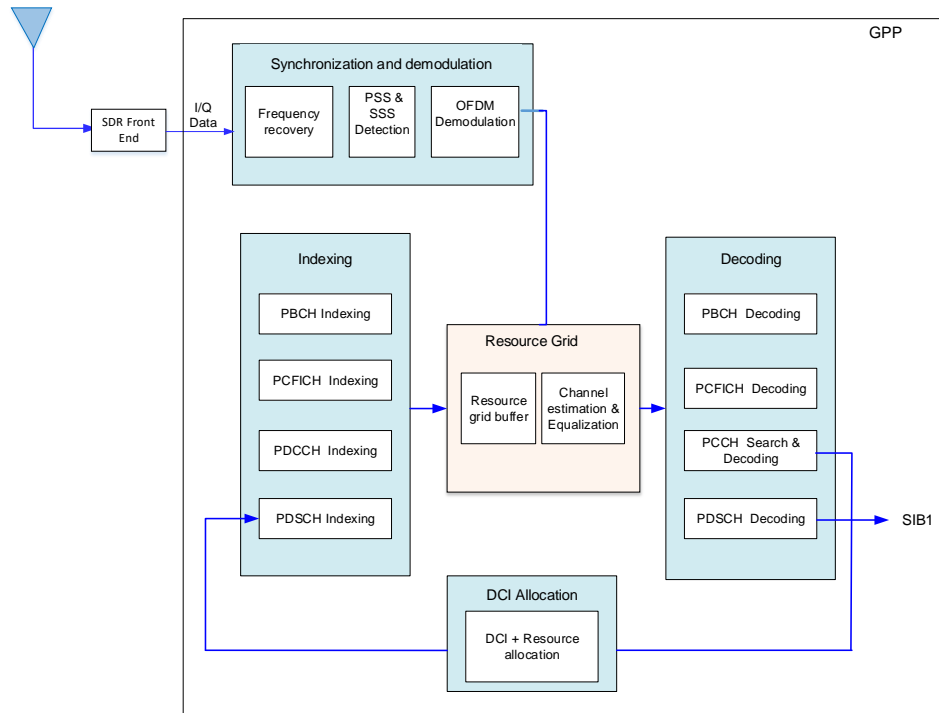


FIG. 8: SYNTHETIC PROCESSING CHAIN OF THE LTE RECEIVER

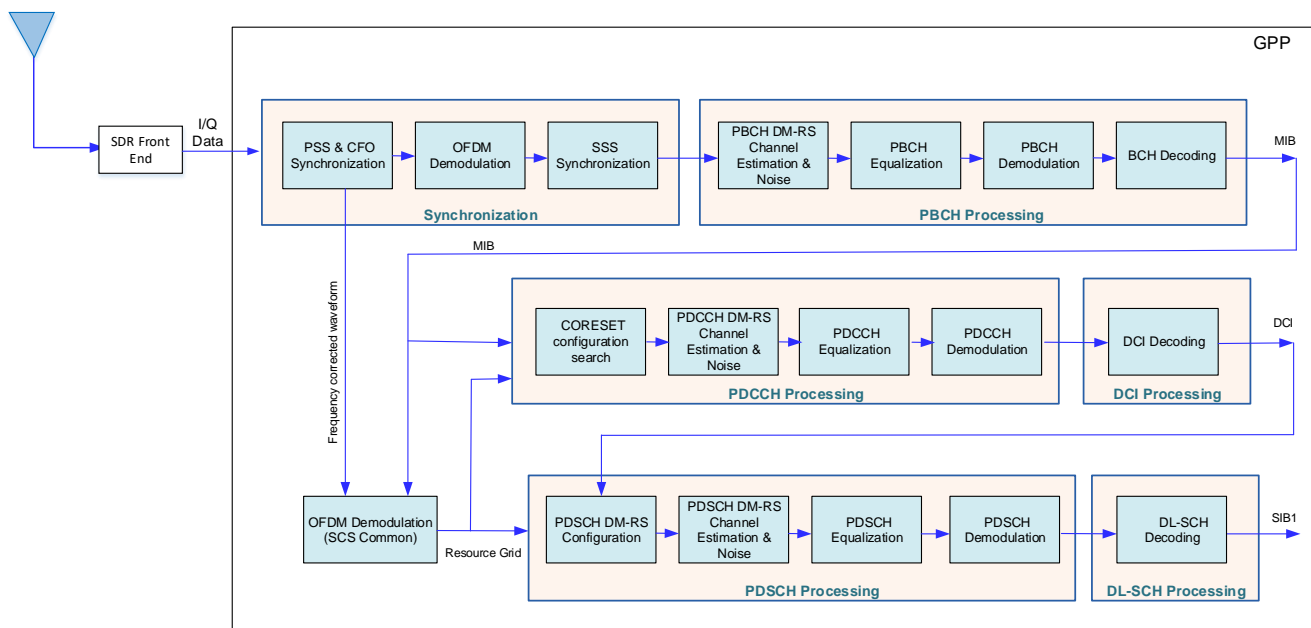


FIG. 9: SYNTHETIC PROCESSING CHAIN OF THE 5G-NR RECEIVER

E. System performance evaluation and validation

The evaluation of the performance of the system which leads to its validation is based on the analysis of various parameters such as the magnitude of the error vector, the adjacent channel leakage ratio or the rate of modulation error (MER). This will also include RF degradation like phase noise as well as timing and frequency offsets on the receiver side. Coarse and fine frequency compensation can then be designed to estimate and compensate for the frequency offset of the received signal. This

assessment is also performed using a multipath fading channel model adapted to the urban environment.

This test compares the over-the-air (OTA) performance of the proposed active wireless device to the performance obtained using the proposed channel model. The principle being firstly to simulate the transmission through the proposed channel model [43]. Secondly, we operate the device in a normal mode by air transmission with real waveforms, to determine the RF

performance of the device under normal use. The comparative analysis focused on the case of the 5G NR receiver because this technology is more demanding in terms of objectives and performance compared to the other two standards (WLAN and LTE).

The paths delays of the channel TDL model are scaled to reach the desired nominal delay spread of 100ns, according to the procedure described in paragraph 7.7.3 of [44]

TABLE 3: CHANNEL MODEL AND SIMULATION PARAMETERS

Parameter	Description
Frequency bands	FR1
Direction of transmission	Downlink
5G NR reference signals	DL-FRC-FR1-QPSK DL-FRC-FR1-64QAM DL-FRC-FR1-256QAM
Carrier frequency	2.140 GHz (n_1 band)
Bandwidth	10MHz
Subcarrier spacing	15kHz
Duplex mode	FDD
Channel model	TDL with Suzuki distribution for path gains
Delay spread	Nominal value of 100ns for 24 taps [44]
Path gains	Generated using the channel model presented in [43][45]
Equalization	MMSE
Mobile speed	50Km/h

Fig. 10 shows the different setup for testing.

III. RESULTS

The screenshots show the power measurement of the channel and the ACLR combined with a display of the constellation and measurements of the vector signal quality of the M-PSK or M-QAM signals. The curves associated with the primary synchronization signal (PSS) as well as the secondary synchronization signal (SSS) allow a correction of the frequency and time shifts of the signal while providing the values of these time and frequency errors. They also allow to calculate the cell identifier in the LTE and 5G NR cases.

In all cases, modulation is automatically detected using blind detection for the packets and is displayed as a constellation. The data synthesis then indicates the values of the EVM, the MER, as well as a measure of the signal strength.

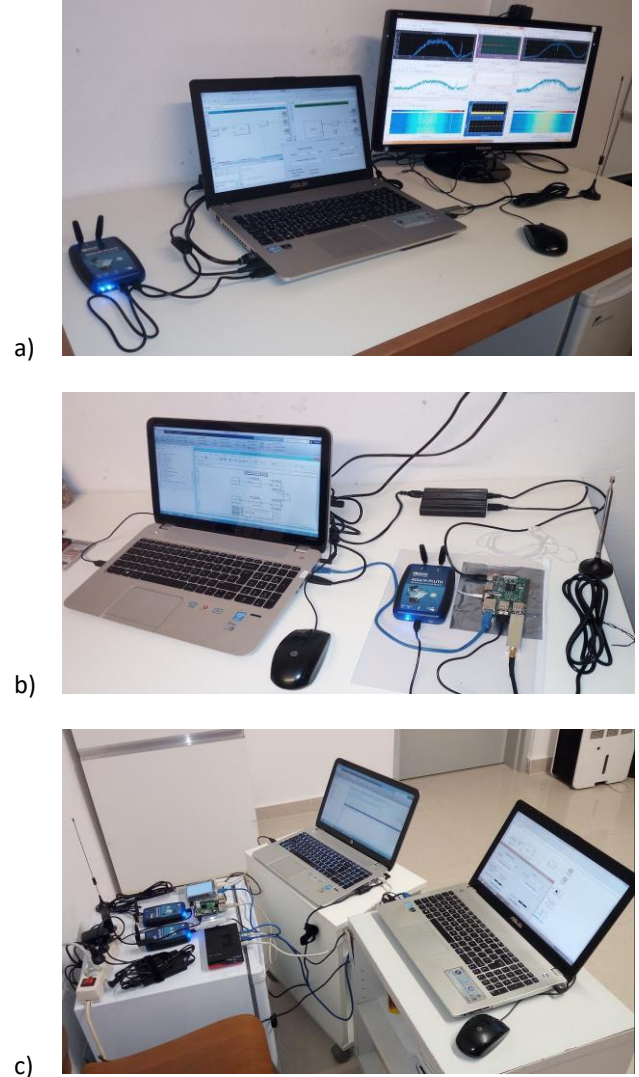


FIG. 10: RECEIVER TEST: A) GENERIC PC AND RF FRONT-ENDS SUPPLIED BY THE RTL-SDR MODULE AND ADALM PLUTO, B) RASPBERRY PI 3B + AND RF FRONT-ENDS SUPPLIED BY ADALM PLUTO AND RTL-SDR MODULES AND C) TEST OF TWO INDEPENDENT SYSTEMS

A. WLAN transceiver

The spectrum of the Non-HT WLAN signal generated and transmitted is shown in Fig. 11 below. The case of the modulation and coding scheme MCS = 4 is given here as an indication. As can be seen, we are dealing with a 20MHz bandwidth signal. The signal is centered on the 2.432MHz carrier frequency which corresponds to WLAN channel 5. The main results are shown in Table 4 as well as in various figures (Fig. 11 to Fig. 13)

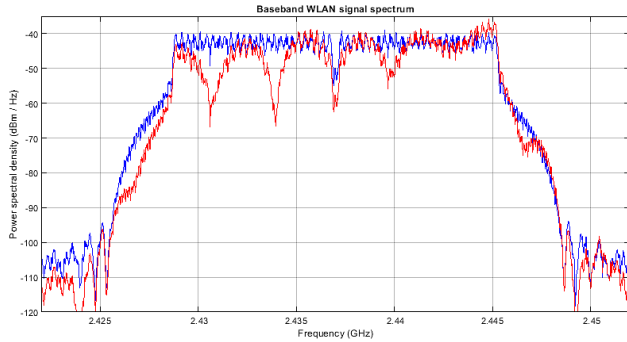


FIG. 11: SPECTRA OF THE TRANSMITTED (BLUE) AND RECEIVED (RED) WLAN SIGNAL

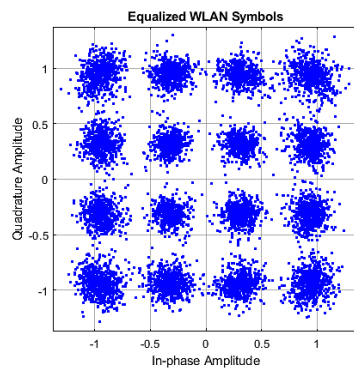


FIG. 12: CONSTELLATION SHOWING EQUALIZED SYMBOLS

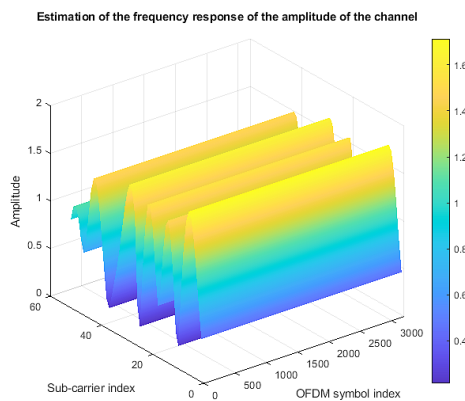


FIG. 13: ESTIMATION OF THE FREQUENCY RESPONSE OF THE CHANNEL

TABLE 4: WLAN SIGNAL QUALITY RESULTS BASED ON MCS

MCS	EVM RMS (%)	MER (%)	Timing Offset (Samples)	Frequency Offset (kHz)
2	7.91	18.32	124030	4.155
3	6.91	19.58	76813	4.136
4	7.13	19.13	64425	4.030
5	9.18	16.95	38097	4.243
6	7.97	18.04	33243	4.626
7	6.29	20.29	26358	4.619

B. LTE transceiver

Table 5 below summarizes the signal quality results for the considered LTE reference measurement channels. In addition,

various curves (from Fig. 14 to Fig. 18) make it possible to better appreciate these results and therefore to better interpret them.

TABLE 5: LTE SIGNAL QUALITY RESULTS BASED ON RMC CHANNEL

RMC	EVM RMS (%)	MER (%)	Timing Offset (Samples)	Frequency Offset (kHz)
R.2	2.77	27.57	8365.00	4.528
R.3	2.92	27.07	64007.00	5.127
R.4	6.52	20.31	13334.00	5.148
R.5	7.00	22.83	20129.00	4.516
R.6	2.14	29.73	20358.00	4.415
R.9	4.19	23.87	67148.00	4.395

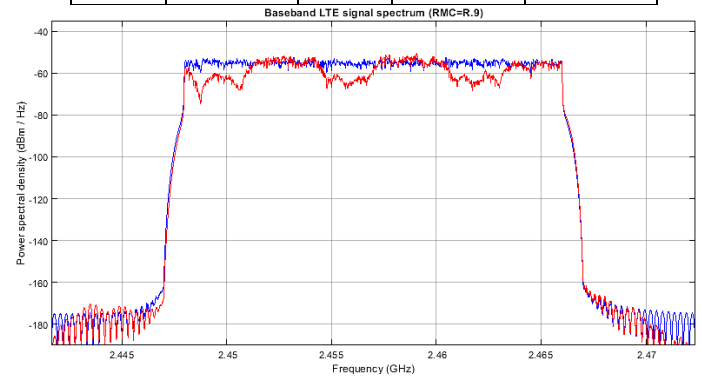


FIG. 14: TRANSMITTED (BLUE) AND RECEIVED (RED) LTE SIGNAL SPECTRA FOR RMC=R.9

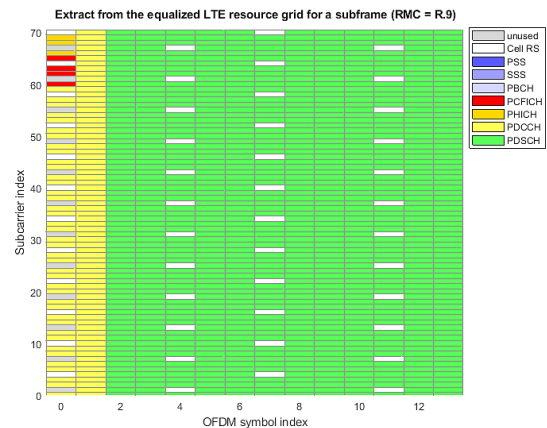


FIG. 15: RECEIVED LTE SIGNAL GRID FOR A SUBFRAME (RMC = R.9)

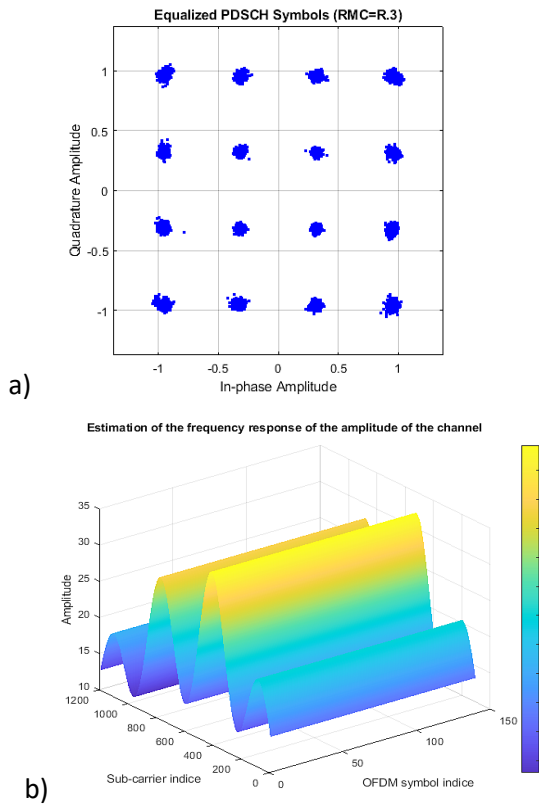


FIG. 16: A) RECEIVED PDSCH CONSTELLATION AND B) CHANNEL AMPLITUDE FREQUENCY RESPONSE FOR RMC = R.3

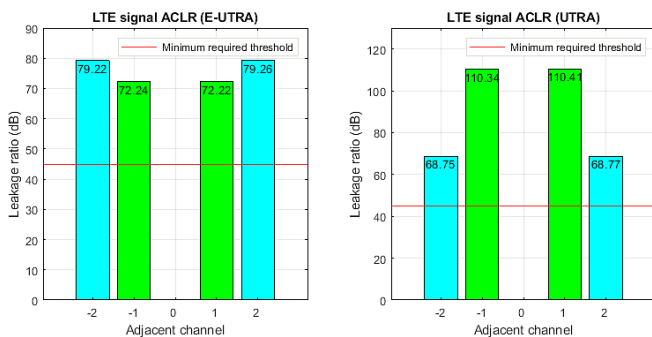


FIG. 17: ACLR AT TRANSMITTER LEVEL

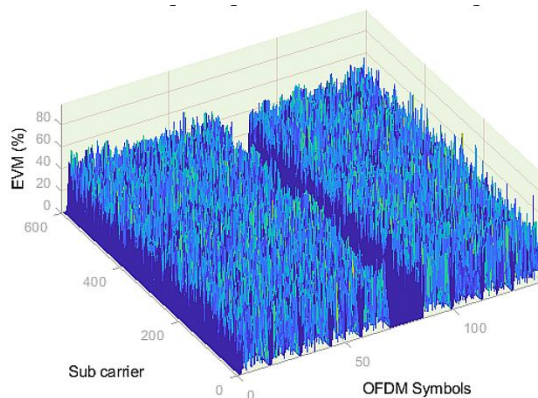


FIG. 18: EVM AGAINST VARIOUS PARAMETERS FOR RMC = R.3

A measurement of the leakage rate in the adjacent E-UTRA and UTRA channels for the different reference channels and therefore different rates and modulation schemes, with ambient noise compensation, is carried out in order to evaluate the spectral efficiency of the transmitter. The results are available in Table 7.

C. 5G NR transceiver

The results for the 5G NR transceiver can be seen below. (From Fig. 19 to Fig. 23 as well as Table 6).

TABLE 6: 5G NR SIGNAL QUALITY RESULTS BASED ON FRC CHANNEL

FRC	EVM RMS (%)	MER (%)	Timing Offset (Samples)	Frequency Offset (kHz)
DL-FRC-FR1-QPSK	0.87	1.39	1212722	6.548
DL-FRC-FR1-64QAM	0.87	1.18	1186453	7.073
DL-FRC-FR1-256QAM	0.85	1.18	2273388	-5.348

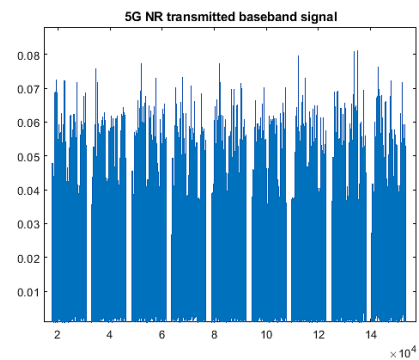


FIG. 19: TRANSMITTED 5G NR BASEBAND SIGNAL

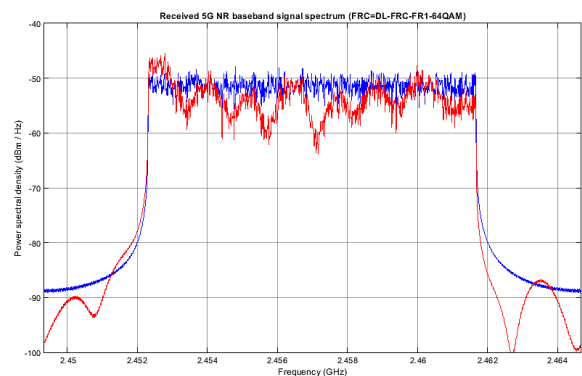


FIG. 20: TRANSMITTED (BLUE) AND RECEIVED (RED) 5G NR SIGNAL SPECTRA

TABLE 7: LTE QUALITY RESULTS (ACLR) BASED ON RMC CHANNEL

RMC	ACLR EUTRA-2	ACLR EUTRA-1	ACLR EUTRA-0	ACLR EUTRA+1	ACLR EUTRA+2	ACLR UTRA-2	ACLR UTRA-1	ACLR UTRA-0	ACLR UTRA+1	ACLR UTRA+2
R.2	78.77	53.4	0	62.85	79.04	67.34	53.02	0	59.53	68.71
R.3	78.74	53.71	0	63.15	79.04	68.66	53.58	0	63.47	68.79
R.4	87.94	62.15	0	62.05	68.24	82.48	70.32	0	69.84	81.59
R.5	84.85	70.42	0	70.49	84.85	88.64	70.28	0	70.28	88.65
R.6	78.88	63.73	0	63.7	78.92	69.52	60.16	0	59.36	69.23
R.9	78.48	59.58	0	60.8	79.15	68.16	58.71	0	61.17	70.51

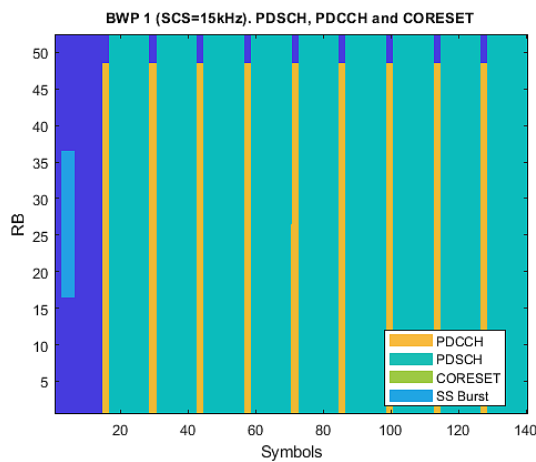


FIG. 21: RECEIVED 5G NR RESOURCE GRID

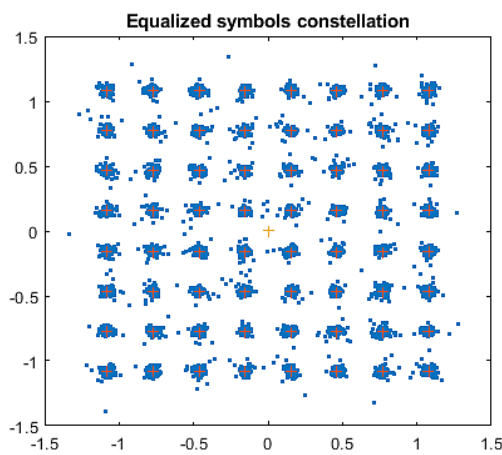


FIG. 22: PDSCH CONSTELLATION AFTER EQUALIZATION FOR DL-FRC-FR1-64QAM

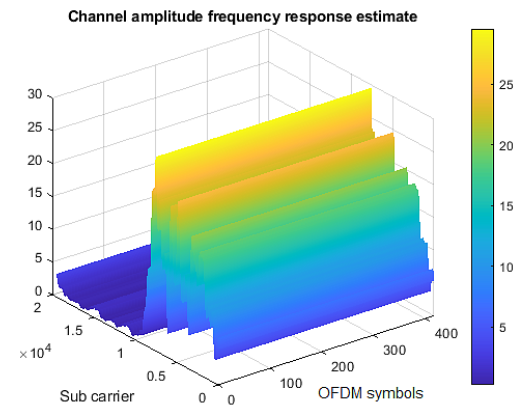


FIG. 23: CHANNEL AMPLITUDE FREQUENCY RESPONSE FOR DL-FRC-FR1-64QAM

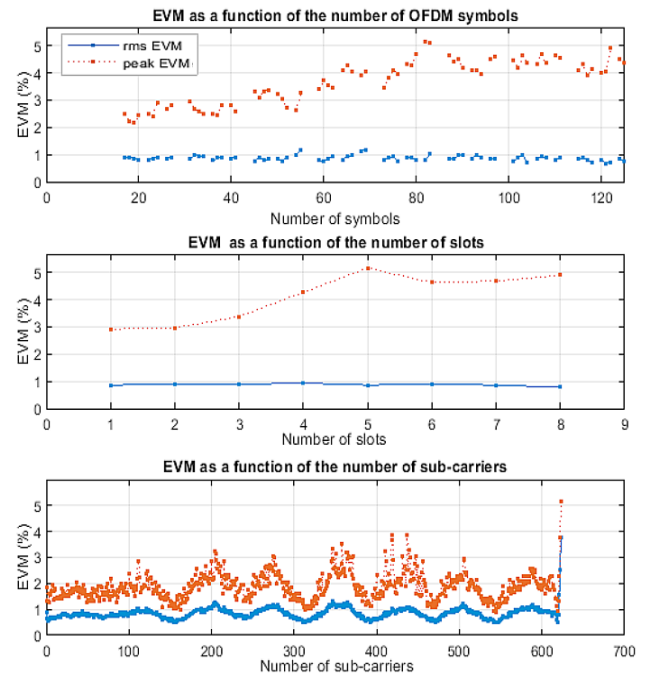


FIG. 24: EVM AGAINST VARIOUS PARAMETERS FOR FRC= 'DL-FRC-FR1-QPSK'

IV. DISCUSSIONS AND ANALYSIS

A. Resource Grid Analysis

One can clearly see the periodic switching of the PDSCH resource allocation over time as well as the PDCCH allocation and other timing signals. For the two LTE and 5G NR standards, we observe a good reconstitution of the grids at the receiver (Fig. 15 and Fig. 21).

B. Spectra and spectral densities analysis

The results show that the signal transmitted has a spectrum with a limited amplitude response, [-110dB, -40dB] for WLAN (Fig. 11), [-180dB, -50dB] for LTE (Fig. 14) and [-100dB, -45dB] for 5G NR (Fig. 20) with a perfect shape, good band limitation as well as a very narrow and noise-free transition band.

LTE and 5G NR technologies present a better spectrum due to the introduction of an FIR filter to improve amplifier response and limit leakage in adjacent channels. In contrast, the spectra of the received signal reflect the effects of the channel's multipath fading response with lower band limitation, wider transition band, more noise and more peaks.

C. Constellation diagrams analysis

Fig. 11 (WLAN), Fig. 15.a (LTE) and Fig. 21 (5G NR) illustrate the constellation diagrams at the receiver for the considered standards. Good symbol recovery can be observed in all three cases as well as the effect of the multipath channel on the signal. Some phase noise can be observed on the 5G NR signal (Fig. 21) but it is clear that the signal processing is correct. The demodulated constellation points exhibit excellent amplitude and phase symmetry for all M-PSK / M-QAM modulation schemes considered.

D. Error Vector Magnitude and Modulation Error Rate analysis

The variation of EVM from local oscillator power levels for different modulation schemes (QPSK, 8PSK, 16PSK, 16QAM and 64QAM) is shown in Fig. 30 to Fig. 32 for the three standards. As observed, the results obtained show acceptable EVM values of less than 10%, for all modulation schemes, in all cases. The EVM is far better because the values are even lower (in the order of 1%) for the case of the 5G NR receiver (Table 6 and Fig. 24). These values of the EVM, clearly prove a low power consumption capacity of the demodulator of the proposed terminal. This makes it possible to reduce the cost of multistandard receivers.

The measured overall EVM values always comply with the requirements of TS 38.104. This proves the capacity of the proposed terminal to discriminate between amplitude and phase. The diagrams also demonstrate that the SISO OFDM transceiver compensates well for the multipath fading effect. Through simulations, we have also carried out another qualitative evaluation with MER performance measurements. This parameter presents acceptable values (MER <21% for the WLAN, MER <30% for the LTE and MER <2% for the 5G NR). The best performances can be observed for the 5G NR case (MER <2%) (Fig. 25 to Fig. 27)

E. Adjacent channel leakage ratio analysis

The minimum ACLR values are obtained for LTE R.2 channels (53.02dB for UTRA and 53.4dB for E-UTRA). On the other hand, the highest values are obtained for channels R.4 and R.5 attesting for better spectral efficiency of the terminal in these latter channels (Fig. 28 and

Fig. 29)

In addition, the impact of the filter has been highlighted in Fig. 30. The ACLR is measured before and after introduction of the FIR filter. We were particularly interested in the first adjacent channels. Before filtering, the minimum ACLR is around 45dB (which is limited compared to the requirements of the standard). After introducing the filter, this value is significantly improved and is around 53dB.

According to TS 38.104, the minimum ACLR required for the measurements conducted is 45 dB and the maximum EVM required when the constellation is 256-QAM is 3.5dB (most critical case) for a 5G NR terminal. The ACLR values for the LTE and 5G NR standards are all greater than 53 dB for both UTRA and E-UTRA channels. This is clearly higher than the 45dB required by the standard. The two measurements therefore comply with the normative requirements.

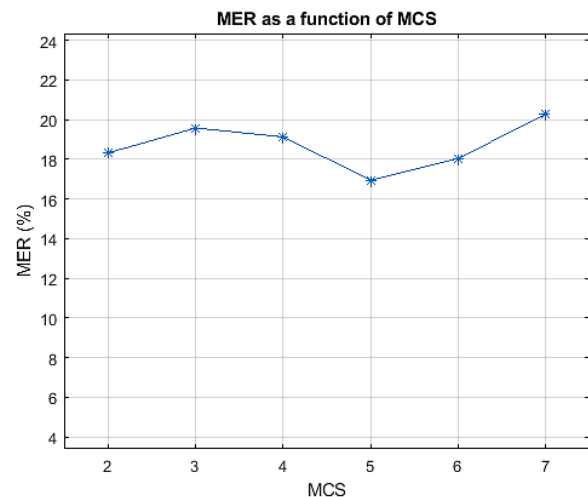


FIG. 25: MODULATION ERROR RATE BASED ON MCS (WLAN)

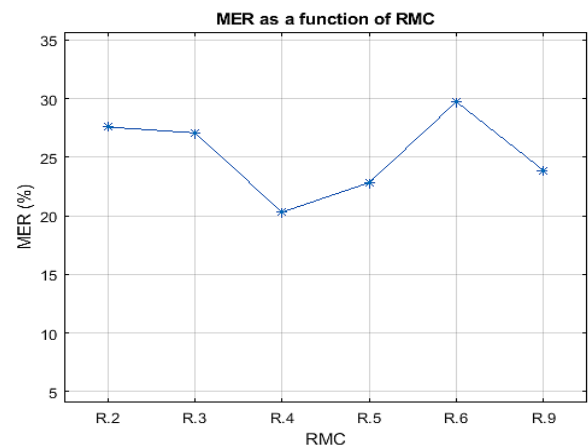


Fig. 26: Modulation error rate based on RMC (LTE)

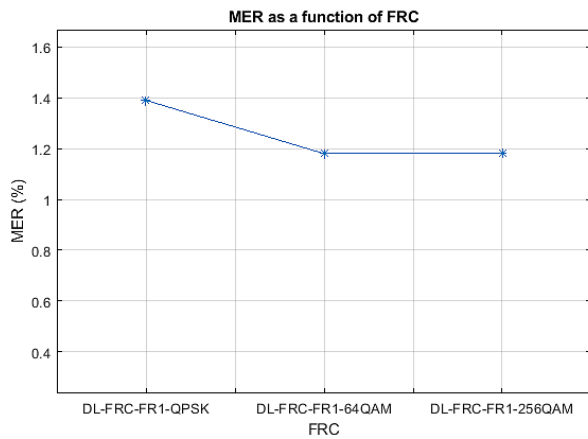


FIG. 27: MODULATION ERROR RATE BASED 5G NR REFERENCE CHANNELS (FRC)

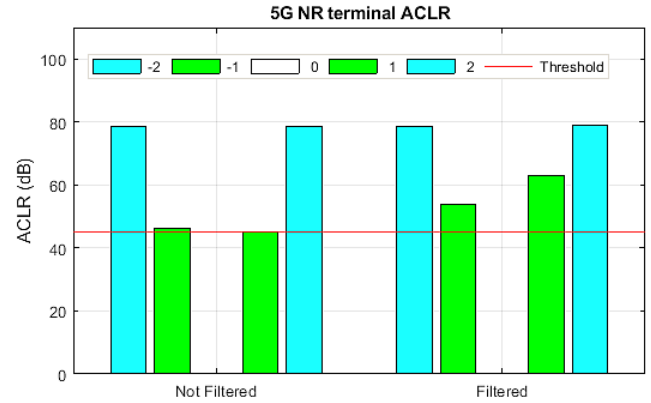


FIG. 30: ADJACENT CHANNELS LEAKAGE RATIO OF THE 5G NR TERMINAL WITHOUT FILTER AND WITH FILTER

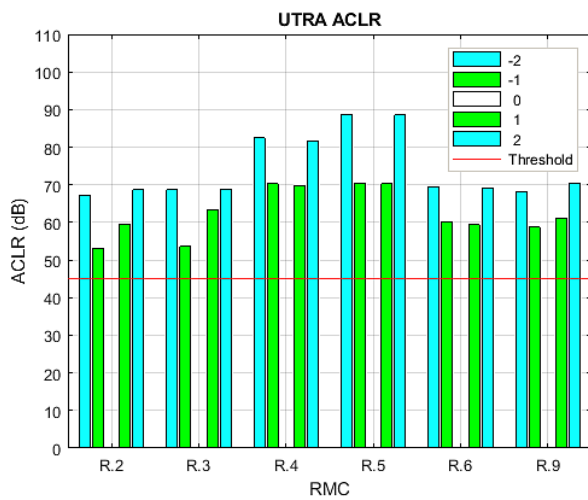


FIG. 28: LEAKAGE RATIO IN UTRA ADJACENT CHANNELS ACCORDING TO THE RMC OF THE LTE TERMINAL

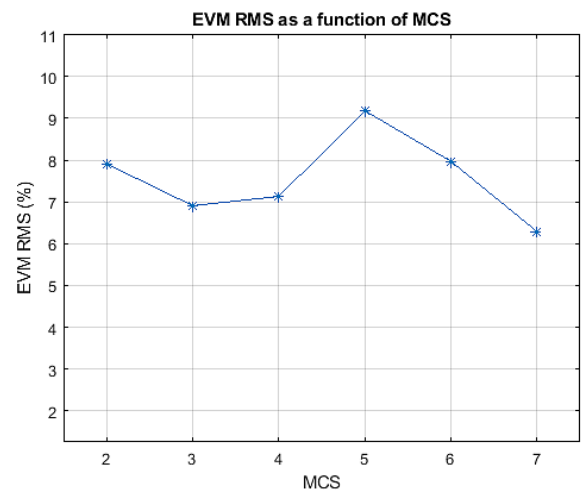


FIG. 31: EVM DEPENDING ON MCS (WLAN)

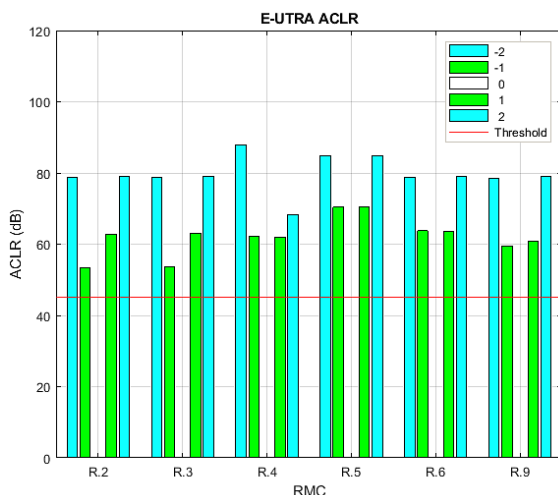


Fig. 29: Leakage ratio in E-UTRA adjacent channels according to the RMC of the LTE terminal

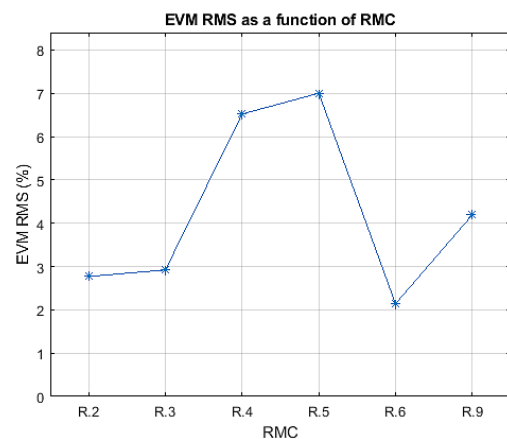


Fig. 32: EVM depending on RMC (LTE)

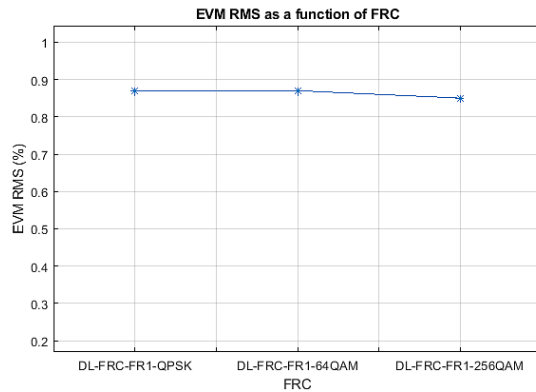


FIG. 33: EVM DEPENDING ON FRC (5G NR)

F. Validation on the proposed channel model

The comparative analysis with the OTA testing mainly focused on the case of the 5G NR receiver because this technology is more demanding in terms of objectives and performance compared to the other two WLAN and LTE standards.

Fig. 34 below shows an illustration of the path gains of our fading channel model.

The results are available in the following table (Table 8):

TABLE 8: 5G NR SIGNAL QUALITY RESULTS OBTAINED THROUGH THE PROPOSED CHANNEL TDL MODEL

FRC	EVM RMS (%)	MER (%)	Timing Offset (Samples)	Frequency Offset (kHz)
DL-FRC-FR1-QPSK	2.97	0.32	1103	62.737
DL-FRC-FR1-64QAM	2.85	0.22	65092	96.857
DL-FRC-FR1-256QAM	2.18	0.50	24694	43.62

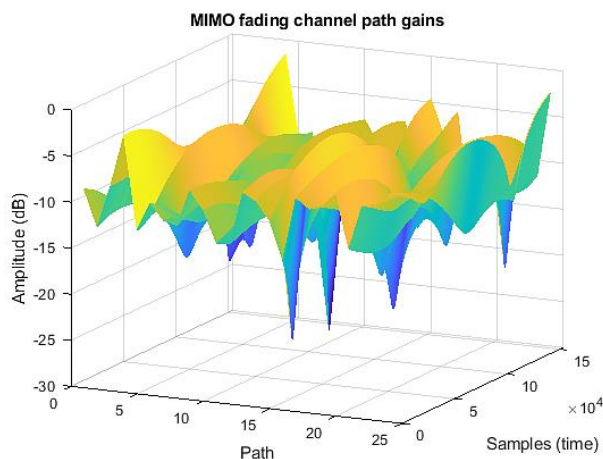


Fig. 34: Path gains of the proposed fading channel model

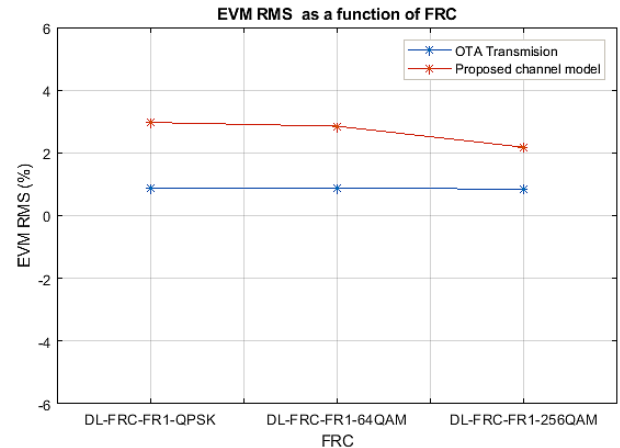


FIG. 35: PERFORMANCE COMPARISON (EVM) BETWEEN OTA TRANSMISSION AND PROPOSED CHANNEL MODEL.

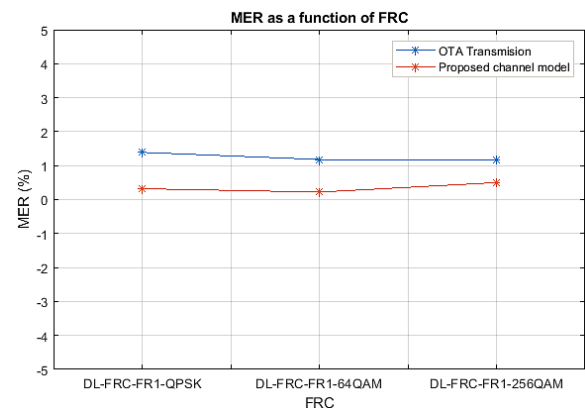


FIG. 36: PERFORMANCE COMPARISON (MER) BETWEEN OTA TRANSMISSION AND PROPOSED CHANNEL MODEL.

The difference for the EVM is of the order of 1% to 2% (Fig. 35) while it is of the order of 0.5% to 1% for the modulation error rate (Fig. 36). The maximum difference in both cases is observed for the DL-FRC-FR1-QPSK reference channel while the minimum difference is observed for the DL-FRC-FR1-256QAM channel. These very satisfactory results attest to the consistency of the channel model as well as the architecture of the software radio terminal proposed.

V. CONCLUSION

A new multistandard receiver architecture was proposed, more suited to the new radio as it exploits the possibilities of software-defined radio. Then followed the validation by performance analysis. The proposed transceiver model integrates LTE, WLAN and 5G wireless systems which are defined in compliance at the physical layer level with the specifications of the latest 3GPP standards. It is built around a GPP such as the Raspberry Pi 3B +for standalone operation, ADALM PLUTO modules and an RTL-SDR. The architecture validation was performed on the proposed channel model and on real waveforms of the three selected standards.

To assess the quality of demodulation and the performance limits of this structure, two studies were carried out. In the first, various demodulation results of M-PSK and M-QAM signals

of WLAN, 4G-LTE and 5G NR standards are presented while, in the second, various diagrams and signal quality measurements such as error vector magnitude, modulation error rate, adjacent channel leakage ratio as well as timing and frequency offsets were evaluated and analyzed. Very good demodulation performances were obtained for all the M-PSK and M-QAM signals considered, again confirming the high potential of the proposed architecture for present and future short-range and high-speed wireless communication systems, including the promising 5G technology.

REFERENCES

- [1] J. P. Delahaye, G. Gogniat, C. Roland, P. Bomel. *Software Radio and dynamic reconfiguration on a DSP/FPGA platform*. FRE, CNRS PY. May 2004.
- [2] Mohamed A. Dahab, Khaled A. Shehata, Salwa H. El Ramly, Karim A. Hamouda. *FPGA Prototyping of Digital RF Transmitter Employing Delta Sigma Modulation for SDR*. 26th National Radio Science Conference, NRSC'2009. Future University, 5th Compound, New Cairo, Egypt, March 17 – 19, 2009.
- [3] Robert W. Stewart, Kenneth W. Barlee, Dale S.W. Atkinson, Louise H. Crockett, David Crawford, Iain Chalmers, Mike McLernon, and Ethem Sozer. *A Low-Cost Desktop Software Defined Radio Design Environment Using MATLAB, Simulink, and the RTL-SDR*. IEEE Communications Magazine 53(9):64-71. September 2015
- [4] Ahmad Ali Tabassam, Farhan Azmat Ali, Sumit Kalsait, Muhammad Uzair Suleman. *Building Software-Defined Radios in MATLAB Simulink - A Step Towards Cognitive Radios*. 2011 UKSim 13th International Conference on Modelling and Simulation. IEEE.
- [5] J. Mitola, *Software Radios Survey, Critical Evaluation and Future Directions*. In Telesystems Conference, NTC. National, (Washington, DC, USA), pp. 13/15 – 13/23, IEEE, 1992.
- [6] Mickael Dardaillon, Kevin Marquet, Tanguy Risset, Antoine Scherrer. *Software Defined Radio Architecture Survey for Cognitive Testbeds*. Université de Lyon, Inria, INSA-Lyon, CITI, 2012 IEEE.
- [7] Amiya Karmakar, Amrita Saha, and Amitabha Sinha. *On the Design of a Reconfigurable Radio Processor Using FPGA*. International Journal of Computer Theory and Engineering, Vol. 6, No. 2, April 2014.
- [8] Laurent Alaus. *Architecture Reconfigurable pour un Equipement Radio Multistandard*. These de Doctorat en Traitement du Signal et Telecommunications. Université de Rennes I. Mai 2010
- [9] Kevin Skey, John Bradley, Karl Wagner. *A Reuse Approach for FPGA-based SDR Waveforms*. The MITRE Corporation Bedford, MA. 2007
- [10] Amor Nafkha, Renaud Segulier, Jacques Palicot, Christophe Moy, Jean-Philippe Delahaye. *A Reconfigurable Baseband Transmitter for Adaptive Image Coding IETR/Sup'elec - Campus de Rennes*, 2007
- [11] Emilie Avignon. *Contribution a la conception d'un modulateur Sigma-delta passe-bande a temps continu pour la conversion directe de signaux radiofréquences*. These de Doctorat en Electronique. Université Pierre et Marie Curie. Decembre 2007
- [12] Martha Liliana Suarez Penaloza. *Architectures d'émetteurs pour des systèmes de communication multi-radio*. These de Doctorat en Electronique, Optronique et Systèmes. Université de Paris Est. Decembre 2009.
- [13] Ali Beydoun. *Système de numérisation a haute performances a base de modulateurs Sigma-Delta passe-bande*. These de Doctorat En Sciences, Option electronique. Université Paris XI Orsay. Mai 2008
- [14] Mehmet Sonmez, Ayhan Akbal. *FPGA-Based BASK and BPSK Modulators Using VHDL: Design, Applications and Performance Comparison for Different Modulator Algorithms*. International Journal of Computer Applications (0975 – 8887) Volume 42– No.13, March 2012.
- [15] Ioan Burciu. *Architecture de récepteurs radiofréquences dédiés au traitement bibande simultané*. These de Doctorat. Ecole Doctorale Electronique, Electrotechnique, Automatique de l'Institut National des Sciences Appliquées de Lyon. Mai 2010
- [16] Mazen Youssef. *Modélisation, simulation et optimisation des architectures de récepteur pour les techniques d'accès W-CDMA*. These de Doctorat. Ecole Doctorale IAEM – Lorraine. Université Paul Verlaine – Metz. Juin 2009
- [17] Sanket Prakash Joshi. *Integrating FPGA with Multicore SDR Development Platform to Design Wireless Communication System*. Thesis for the Degree of Masters of Science in Electrical Engineering. California State University, Northridge. May 2012
- [18] Haisheng Liu. *Contributions à la maîtrise de la consommation dans des turbo-décodeurs*. These de Doctorat en Sciences de l'Ingenieur. Telecom Bretagne-Université de Bretagne Sud. Juillet 2009
- [19] Ruben Bartholomä, Frank Kessel. *Implementing Signal Processing Algorithms on FPGAs*. University of Applied Sciences Pforzheim, Germany. 2003
- [20] Debyo Saptano. *Conception d'un outil de prototypage rapide sur le FPGA pour des applications de traitement d'images*. These de Doctorat en Instrumentation et Informatique de l'Image. Université de Bourgogne. Novembre 2011
- [21] Guangye Tian. *Flot de Conception Système sur Puce par Radio Logicielle*. These de Doctorat en Informatique. Université de Paris Sud 11. Juillet 2011
- [22] Michaël Grand. *Conception d'un cryptosystème reconfigurable pour la radiologique sécurisée*. These de Doctorat en Electronique. Université de Bordeaux 1. Decembre 2011
- [23] Eric Batut. *Etude du bloc de réception dans un terminal UMTS-FDD et développement d'une méthodologie de codesign en vue du fonctionnement en temps réel*. These de Doctorat. Institut National Polytechnique de Grenoble. Juin 2002
- [24] Chris H Dick, Henrik M Pedersen. *Design and Implementation of High-Performance FPGA Signal Processing Datapaths for Software Defined Radios*. Article
- [25] Riadh Ben Abdallah. *Machine Virtuelle Pour La Radio Logicielle*. These de Doctorat en Mathématiques et Informatique. INSA de Lyon. Octobre 2010.
- [26] Khalid El Tahir Mohamed Osman. *Development of a multi standard protocol using Software Defined Radio for a mobile station transceiver*. Doctor of Philosophy Thesis. Universiti Putra Malaysia, March 2009
- [27] Loïc Godard, Christophe Moy, Jacques Palicot. *From a Configuration Management to a Cognitive Radio Management of SDR Systems*. CrownCom'06 – First International Conference on Cognitive Radio Oriented Wireless Networks and Communications. 2006
- [28] Antonio Di Stefano, Giuseppe Fiscelli, Costantino G. Giaconia. *An FPGA-Based Software Defined Radio Platform for the 2.4GHz ISM Band*. Università degli Studi di Palermo. 2006 IEEE.
- [29] Yahong Rosa Zheng and Chengshan Xiao. *Simulation Models With Correct Statistical Properties for Rayleigh Fading Channels*. IEEE Transactions on communications, Vol 51 No 6, June 2003.
- [30] Robert W. Stewart, Kenneth W. Barlee, Dale S.W. Atkinson, and Louise H. Crockett. *Software Defined Radio using MATLAB & Simulink and the RTL-SDR*. Strathclyde Academic Media. ISBN 978-0-9929787-2-3. 2017.
- [31] Lavanya T, 2Natraj URS HD. *Design and Implementation of FM modem on FPGA for SDR using Simulink*. International Journal of Recent Advances in Engineering & Technology (IJRAET). Volume-4, Issue - 9, 2016.
- [32] Ankit Kumar RS. Gupta & Tejas Sanjay Bodhe. *Design of Software Defined AM radio receiver*. Imperial Journal of Interdisciplinary Research (IJIR) Vol-2, Issue-6, 2016.
- [33] Noori BniLam, Dennis Joosens, Jan Steckel, Maarten Weyn. *Low Cost AoA Unit for IoT Applications*. Flemish FWO SBO S004017N IDEAL-IoT (Intelligent Dense And Long range IoT networks)
- [34] Gianni Pasolini, Flavio Zabini, Alessandro Bazzi, Stefano Olivieri. *A Software Defined Radio Platform with Raspberry Pi and Simulink*. 24th European Signal Processing Conference (EUSIPCO). 2016
- [35] IEEE Std 802.11ac™. *IEEE Standard for Information technology - Telecommunications and information exchange between systems - Local and metropolitan area networks - Specific requirements - Part 11: Wireless LAN Medium Access Control (MAC) and Physical Layer (PHY) Specifications - Amendment 4: Enhancements for Very High Throughput for Operation in Bands below 6 GHz*. 2013
- [36] 3GPP TS 36.101. *Evolved Universal Terrestrial Radio Access (E-UTRA); User Equipment (UE) Radio Transmission and Reception*. 3rd Generation Partnership Project; Technical Specification Group Radio Access Network. URL: <https://www.3gpp.org>.
- [37] 3GPP Technical Specification Group Radio Access Network. *NR Base station conformance testing, Part 1: Radiated conformance testing, Release 16; 3GPP TS 38.141-1, V16.3.0*. 2020. Available: <https://www.3gpp.org/DynaReport/37941.htm>

-
- [38] 3GPP Technical Specification Group Radio Access Network. *NR Base station conformance testing, Part 2: Radiated conformance testing*. Release 17; 3GPP TS 38.141-2, V17.0.0, (2020-12) Available: <https://www.3gpp.org/DynaReport/38141-2.htm>
- [39] 3GPP TS 26.132. *Speech and video telephony terminal acoustic test specification*. 3rd Generation Partnership Project; Technical Specification Group Services and System Aspects; V12.8.0 (2016-03) URL: <https://www.3gpp.org>.
- [40] Sebastian-Ioan ENE. *A base station system study for LTE, UMTS and GSM/EDGE*. Delft University of Technology. 2011
- [41] Dr. Oliver Werther/Roland Minihold. *LTE: System Specifications and Their Impact on RF & Base Band Circuits*. Application Note. Rohde&Schwarz 04.2013 – 1MA221_0E.
- [42] ETSI TS 138 101-2 V15.0.0. *5G; NR; User Equipment (UE) radio transmission and reception; Part 1: Range 1 Standalone*. (3GPP TS 38.101-1 version 17.0.0 Release 17) Technical specification (2020-12)
- [43] Michel Mfeze, Emmanuel Tonye. *Comparative Approach of Doppler Spectra for Fading Channel Modelling by the Filtered White Gaussian Noise Method*. International Journal of Computer Science and Telecommunications, Volume 6, Issue 11, December 2015.
- [44] TR 38 901. *Study on channel model for frequencies from 0.5 to 100 GHz* (Release 16). Technical Report V16.1.0, 3GPP. 2019-12
- [45] Michel Mfeze, Emmanuel Tonye. *An Efficient FWGN-Based Modelling And Simulation Scheme For The Suzuki Flat Fading Channel*. IOSR Journal of Electronics and Communication Engineering (IOSRJECE) Volume 13. Issue 2 (April 2018): 40-60.